

Paper n. 331

**Test on the Performance of Resistive Plate Chambers in  
View of Their Use at the LHC  
(Bari - Pavia Collaboration)**

M. Abbrescia, A. Colaleo, G. Iaselli, F. Loddo, M. Maggi, B. Marangelli,  
S. Natali, S. Nuzzo, G. Pugliese, A. Ranieri, F. Romano  
Dip. di Fisica dell'Università and Sezione INFN - Bari, I-80100 Bari, Italy

V. Arena, G. Bonomi, G. Gianini, M. Merlo, S. P. Ratti, C. Riccardi,  
L. Viola, P. Vitulo  
Dip. di Fisica Nucleare e Teorica dell'Università and INFN - Pavia, I-27100 Pavia, Italy

**Abstract**

The Resistive Plate Chambers (hereafter RPC) are part of the muon trigger for the large LHC experiments and they have to work in an environment which is new compared to those of cosmic ray or present accelerator experiments. We report on the behaviour of several double gap bakelite RPCs in several different conditions. In particular we studied:

- the performance of RPCs -operated in streamer mode- without linseed oil treatment of the internal electrodes (efficiency, collected charge and cluster size distributions) compared to those of standard oiled RPCs;
- efficiency in cosmic rays detection and development of its charge in the 2 mm gas gap of an RPC - operated in avalanche mode- under a  $Cs^{137}$  source irradiation. This was done for two different gas mixtures: one containing a high percentage of environmental friendly "freon"  $C_2H_2F_4$ ; another containing a high percentage of argon gas;
- some properties of a 90%  $C_2H_2F_4$  gas mixture used to operate RPCs -in avalanche mode- compared to the predictions of simple analytical calculations and a Montecarlo simulation;
- the performance of several RPCs in muon and pion beams in different running conditions.

These results are extrapolated to the conditions expected at LHC.

# 1 Introduction

Over the last few years a considerable amount of work has been performed in the RPCs field[1], related to the need for a good operation in the LHC environment.

Leading order problems are mostly solved: results on high rates capability with non ozone depleting gas mixtures[2] are now available and they confirm the good behaviour of these detectors.

Recently, concerns have been raised about the following issues:

- a)- the need of a linseed oil electrodes treatment which was introduced many years ago[3] to reduce the dark current of these detectors, at that time operated in streamer mode[4];
- b)- the rate capability advantages offered by an operation of the R. P. C. in avalanche mode[5],[4]d which implies low gas gain, temporal limits as well as consequences on efficiency and signal amplification;
- c)- the most convenient gas mixture to be used for the R. P. C. operation, mostly related to the use of argon vs. freon.

In this report we separately address these points and finally compare some data obtained with different gases to the prediction of simple analytical calculations as well as to the results of Montecarlo simulations.

# 2 Linseed oil treatment

In this section we systematically study how the linseed oil treatment of the electrodes affects the performance of the RPC chambers.

The concerns are mainly two: a- the oil treatment results is a delay time factor when a massive production is involved, as it is the case of LHC experiments (typically several thousands square meters of active areas); b- the heavy ionizing background environment foreseen at LHC requires a careful study of the possible ageing properties and radiation damage of the linseed oil as a chemical compound (this second problem, however, will be not tackled in this paper for sake of brevity).

We compare the behaviour of oiled and non oiled detectors made of bakelite produced with present available technology.

Typical crude linseed oil[6] is a natural organic mixture of mainly linolenic acid (50 – 65 %), linoleic acid (14 – 24 %) and oleic acid (16 – 26 %). It is commonly used, after heating refining, in special paints and coatings. In many commercial products of this type other desiccative metals are added

to guarantee the drying process.

Since the main interest here is the effect of the linseed oil treatment, *only for what concern this section*, the chambers have been operated in streamer mode.

The treatment of the RPC electrodes was done following the traditional procedure by filling the full gas volume of an assembled RPC with linseed oil which is then slowly taken out. The resulting effect is the deposition of a thin layer of oil on both bakelite surfaces facing the gas volume.

It is easy to guess that the oil might have been used to smoothen the surface of the resistive electrodes and that modern technology might produce smoother bakelite sheets which might make the treatment unnecessary.

Let  $y(x)$  be the vertical displacement of a point  $x$  with respect to a given reference plane of quota  $y_o = 0$ ; the "average profile line"  $L_M(x)$  of a longitudinal cut is defined as the one that makes  $\int_{L_{tot}} [y(x) - y_o] dx = 0$ , being  $L_{tot}$  a selected sampling length.

The "average roughness"  $R_a$  is defined as:

$$R_a = \int_{L_{tot}} |y(x) - L_M(x)| dx \quad (1)$$

The comparison between "old" bakelite (made according to the standard technical procedure) and a "new" bakelite (made with improved technology -sheets pressed with stainless steel lapped plates) is shown in fig.1a.

We plot  $R_a$  -in  $\mu\text{m}$ - measured on several sampling points[8]a for the two bakelite sheets. The new production has improved by a factor 5 the value for the "parameter"  $R_a$ , from  $R_a \approx 0.55$  to  $R_a \approx 0.11$  .

The accurate quantitative measurement of the roughness of the surface will be made by measuring fractal (co)dimension[7] of the three-dimensional display of the micropicture of the surface, shown in fig.2.

Good encouraging results (see later) on the chambers performances have been obtained with these new electrodes.

In the following we analyze other operational parameters of non-oiled RPCs operated in streamer mode.

## 2.1 Experimental Setup and Results

Tests have been carried out using 2 mm double gap RPCs, whose cross section is shown in fig. 3.

The detector is made of two gaps with common inner readout aluminum strips (1.3 cm wide). The high voltage (hereafter HV) supply can be applied

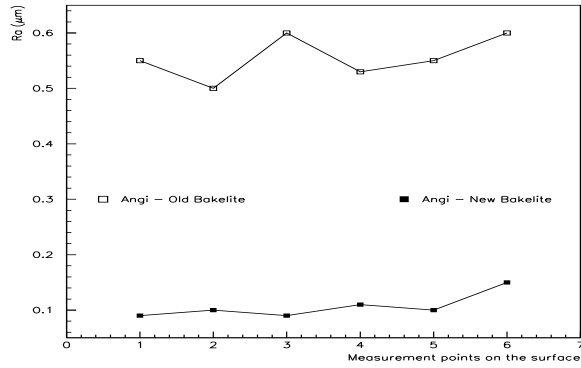


Figure 1: Value of the average roughness  $R_a$  in microns for 6 different random sample points on the surface of bakelite foils. Open squares: "old" bakelite; (production of the late eighties); open circles: "new improved surface" bakelite.

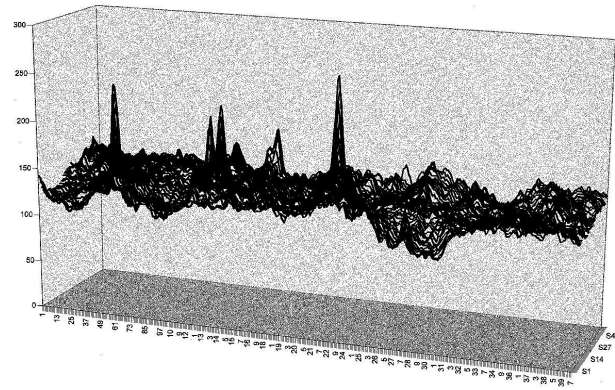


Figure 2: Pixel greyscale readout of a microphotograph -in arbitrary scale- of a piece of "old" bakelite. The pixels are  $0.25\mu m \times 0.25\mu m$  in size. The scanned area is  $100\mu m \times 12\mu m$ .

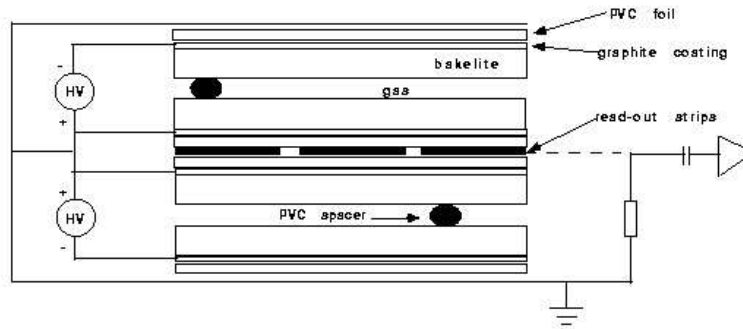


Figure 3: Cross section (not to scale) of a double gap chamber RPC with common strip readout

independently to each gap so that the chamber can be operated either in double gap or single gap mode, by turning off one of the supplies. The area of the detector is  $50 \times 50 \text{ cm}^2$ . The bakelite foils, of resistivity  $0.4 \cdot 10^{11} \Omega\text{cm}$ , are 0.2 cm thick. The RPCs were operated in streamer mode and filled with an argon/isobutane/freon 13B1 (48%/48%/4%) gas mixture.

The experimental setup[8]b consists of a cosmic ray telescope made of 5 horizontal RPCs, 4 of which were not oiled at the beginning. The fifth chamber is a standard (oiled) RPC used as reference detector for the various measurements. The reference chamber is one year old and has been previously used for several tests. Three scintillator counters acting as triggering system define a  $10 \times 10 \text{ cm}^2$  trigger area. The strips are connected at both ends to different electronics to allow simultaneous charge and time measurements. Signals from one end of the strips are input to CAEN C205A Analog Digital Converters (ADCs), with a 0.25 pC channel sensitivity. Signals from the other end have been discriminated and sent to LeCroy 2228A Time Digital Converters (TDCs). Single gaps can be readout by switching off the power supply to the companion gap.

This scheme provides maximal flexibility and allows two independent measurements of the efficiency.

Non-oiled RPCs will be labeled 1 to 4 in fig.s 4-6, while “R” will indicate the standard oiled reference detector. When the detectors are operated in

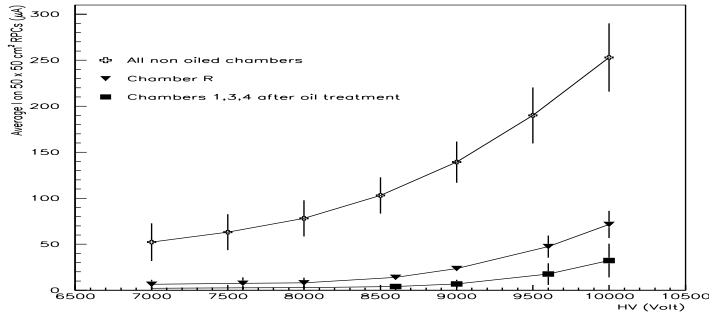


Figure 4: Current vs HV averaged on all non oiled (open cross) and oiled gaps (full square); chamber R behaviour (full triangle) is shown as reference. Error bars correspond to one standard deviation.

single gap mode two additional labels, A and B, are used to identify the gap. The experimental results are summarized in fig.s 4-6

After a month of running, RPCs 1,3 and 4 were treated with linseed oil and a new set of measurements were performed to inspect all possible changes in the behaviour of the detectors.

## 2.2 Currents and Single Rates

Fig. 4 shows the average dark currents of a single gap as a function of HV before and after the oil treatment. The error bars represent  $1.0\sigma$  spread of the currents in the 8 single gaps used separately.

After the treatment of RPCs 1, 3 and 4, the values of the dark currents are, at least, a factor 4 less. For comparison the average currents of the two gaps of the reference chamber are also shown.

Single rates were measured counting the ORed signals from 8 strips. The threshold for non oiled chambers was set to  $-80 mV$ ; to be conservative the threshold for the oiled case was set to  $-50 mV$ .

Fig. 5a shows the average single rate, scaled to a square meter area, for all non oiled gaps. Fig. 5b shows, for comparison, the average OR rate of gaps 1A/B, 3A/B and 4A/B after linseed oil treatment. The behaviour of

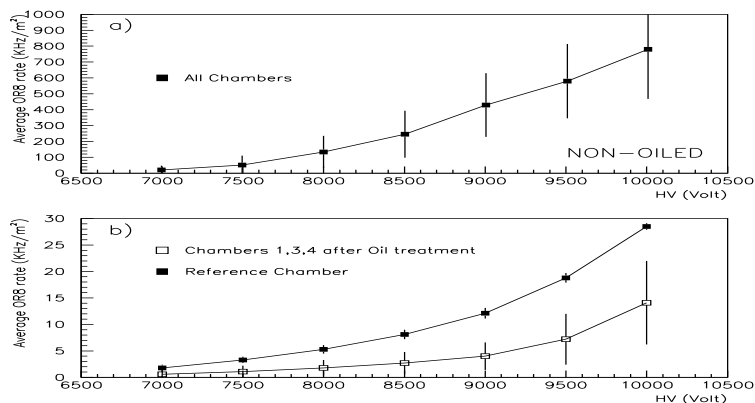


Figure 5: Average single rate (as explained in the text) vs HV at a fixed discriminating threshold: a) Non oiled gaps; threshold  $-80\text{ mV}$ . b) Oiled gaps; threshold  $-50\text{ mV}$ . The chamber R is shown as reference.

the reference chamber is also shown for comparison. In spite of the lower threshold setting, we see that the oil treatment decreases the rate by an order of magnitude. Local rate effects for the non oiled electrodes are also observed, while the local behaviour of the oiled RPCs is more homogeneous.

Efficiencies were calculated from the ADCs information by requiring a charge signal to be present after a certain threshold and after pedestal subtraction. The threshold was set to a  $50\text{ mV}$  signal equivalent; this corresponds to a charge of  $10\text{ pC}$  assuming a triangular shape for the signal,  $20\text{ ns}$  wide at the base and readout on a  $50\ \Omega$  resistor. Since not all the data were available with the TDCs information, we used the charge distributions in the efficiency calculations. This approach might overestimate the efficiency at low HV; however the plateau values are comparable to those obtained with other methods such as TDCs and scalers.

Figs 6a-d (fig. 6a, chamber 1; fig. 6b, chamber 2; fig. 6c, chamber 3; fig. 6d, chamber 4) show the efficiencies for the two gaps A and B of the 4 different chambers - non oiled case - while fig. 6e shows, for comparison, the efficiency for the two gaps A and B of the reference oiled chamber. The

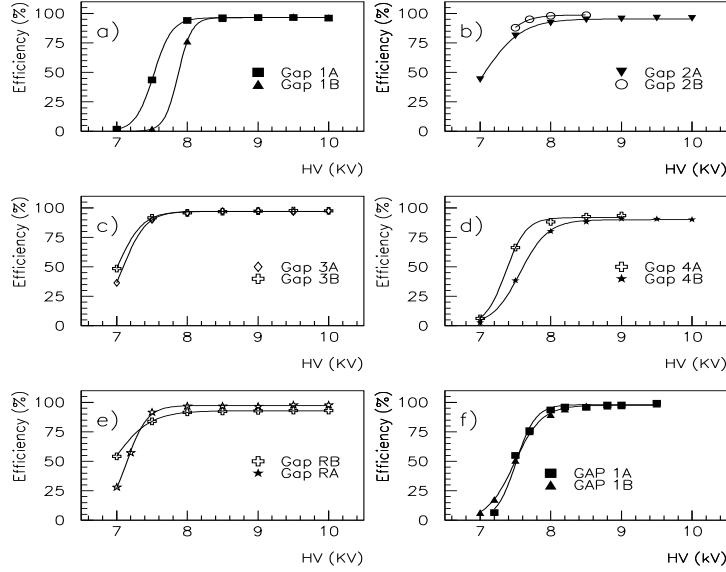


Figure 6: Efficiency vs HV for non oiled gaps (simulated threshold as explained in the text:  $-50\text{ mV}$ ): a) Chamber 1; b) Chamber 2; c) Chamber 3; d) Chamber 4; e) Reference Chamber; f) Chamber 1 after oil treatment.

absence of the surface treatment of the electrodes does not seem to affect the plateau efficiency of the RPCs. In some cases however (fig. 6a and 6d) the knee of the plateau is shifted about  $500\text{ V}$  higher than those of the reference gaps (fig. 6e). For further comparison, fig. 6f shows the efficiency of chamber 1 after oil treatment. The plateau values are left substantially unchanged by the treatment.

We also investigated charge and cluster size distributions. The charge spectrum was obtained by integrating over  $250\text{ ns}$  any analogic signal induced on 14 strips in coincidence with a trigger event, while the cluster size was calculated via TDC information (each discriminated strip signal arriv-

ing within 200 ns from the trigger leading edge contributed to the cluster size distribution). We did not notice any particular difference among the average behaviours.

### 3 Performance with Different Gases under $^{137}\text{Cs}$ Irradiation

When an RPC is operated in an avalanche mode[5] -as will be done from here on in the present paper- rate capability is not an issue anymore [9]; however one has still to compel with two major requirements.

The first requirement is the need of keeping the uncertainty on bunch crossing identification as small as possible (to achieve this target, fast gas mixtures, i.e. mixtures with high electron drift velocity, have to be preferred). Freon based mixtures proved to be a suitable choice which also allows high rate detector operation. The second requirement is provided by the detector power consumption at high rate which, even in presence of low gas amplification, may exceed tolerable limits.

The two requirements are clearly in conflict: on one hand, the use of freon reduces the charge collection time, thus improving the timing; on the other hand its use increases the power consumption, due to its high electronegativity.

Only a small fraction of electrons produced in the avalanche contributes to the signal, the majority of them being attached to freon molecules. It is therefore useful to study the behaviour of non electronegative gas mixtures to see whether they could allow lower power consumption without degrading considerably other performances.

We compare here the behaviour of a double gap RPC module filled with two different gas mixtures and operated under a 0.65 mCu  $^{137}\text{Cs}$  source irradiation. The source simulates a steady background counting rate of about  $500\text{Hz}/\text{cm}^2$  on an area of 10 cm x 10 cm. The two gas mixtures are: a)- 90%  $\text{C}_2\text{H}_2\text{F}_4$  and 10% i- $\text{C}_4\text{H}_{10}$ , an environmental friendly ozone safe gas (hereafter "freon" mixture). b)- 70% argon, 5% i- $\text{C}_4\text{H}_{10}$ , 10%  $\text{CO}_2$  and 15%  $\text{C}_2\text{H}_2\text{F}_4$  (hereafter "argon" mixture).

### 3.1 Experimental setup and results

A  $50 \times 50 \text{ cm}^2$  double 2 mm gap RPC with oiled bakelite plates (operated in avalanche mode) has been used for these measurements. The CR telescope of section 2.1 is substituted by a set of scintillators placed above and below the chamber. A  $^{137}\text{Cs}$  source, placed in the vicinity of the chamber, could be moved to irradiate the chamber at an average counting rate of about  $500 \text{ Hz/cm}^2$  on an area of  $10 \text{ cm} \times 10 \text{ cm}^2$ . The geometry was arranged to cover a single strip. Here, the end of the strips was connected to a LeCroy NIM 612 AM amplifier having voltage gain 40 and bandwidth 140 MHz. The other end was terminated on a  $50 \Omega$  resistor.

The efficiency was measured by means of NIM scalers after 20 mV threshold discrimination, which corresponds about to a 50 fC charge threshold when the signal shape is taken into account. Signals from the strip defined by the trigger coincidence were sent to a Le Croy 300 MHz digital oscilloscope which stores the waveforms on a disk memory for an off-line measurement of the charge and the streamer probability. We define the streamer probability as the fraction of events in which an additional signal with charge at least 10 times larger than the average avalanche charge, appears in a 200 ns time window. Due to the  $50 \Omega$  termination on both ends of the strips, only half of the charge induced on the strip was measured by the system.

Efficiency measurements vs HV, for freon and argon mixtures, in absence of irradiation, are shown in fig.s 7, a and b respectively. In each plot data are given for both single and double gap operation. In the same figures, the streamer probability is also plotted.

The fraction of streamers produced at a given HV is an important parameter to characterize the operation mode of the chamber. According to Crotty et al. [4]d, who consider the streamer probability as a function of the gas gain dynamic range, we can figure out the streamer probability for different gas mixtures.

If we aim at an efficiency in excess of a probability  $P\%$ , using electronics sensitive to a single cluster, with a given detection threshold and a given minimum gas gain, at least one primary cluster must lye, with probability  $P$ , within a maximum distance  $x_{max}$  from the cathode. Therefore, for a double gap RPC:

$$P_1[0, x_{max}] \times P_2[0, x_{max}] = e^{-2\lambda x_{max}} = 1 - P$$

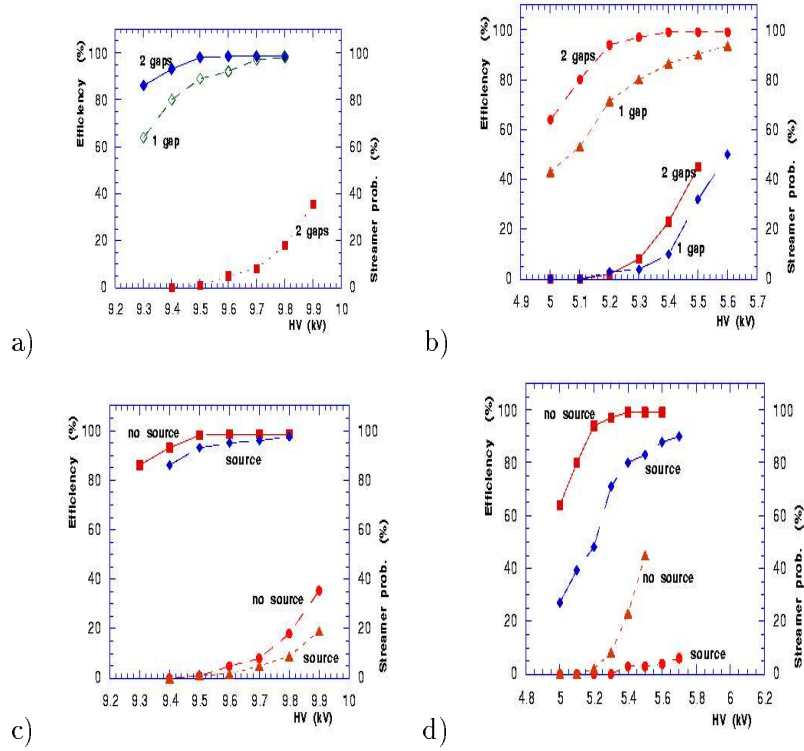


Figure 7: a- efficiency and streamer probability in freon without source; b- efficiency and streamer probability in argon without source; c- comparison of efficiency and streamer probability for double gap operation in freon with and without source; d- Comparison of efficiency and streamer probability for double gap operation in argon with and without source.

where  $P_i[\cdot]$  is the probability that, in the gap  $i$ , no clusters are found within  $x_{max}$  from the cathode, and  $\lambda$  is that cluster density mixture. Thus:

$$x_{max} = -\frac{\ln(1 - P)}{2\lambda}$$

and the dynamic range is:

$$R = \frac{e^{\eta d}}{e^{\eta(d-x_{max})}} = e^{\eta x_{max}}$$

the denominator being the given threshold,  $\eta$  the effective Townsend coefficient and  $d$  the gap width. With another mixture, having cluster density  $\lambda'$ :

$$R' = \frac{e^{\eta' d}}{e^{\eta'(d-x'_{max})}} = e^{\eta' x'_{max}}$$

From the threshold equality:

$$\eta' = \eta \frac{d - x_{max}}{d - x'_{max}}$$

one sees that when  $\lambda' < \lambda$ , then  $R' > R$ . For example with  $P = 95\%$ ,  $d=2$  mm,  $\lambda = 5 \text{ mm}^{-1}$  (typical for freon mixtures),  $\lambda' = 2.5 \text{ mm}^{-1}$  (typical for argon mixtures),  $\eta = 9$ , we have  $R = 15$ ,  $R' = 704$ . The use of light gases increases the streamer probability. As already outlined by Crotty et al.[4], the use of wider gaps is in such a case mandatory.

Figs 7 show that, below a given HV (9500 V in freon, 5200 V in argon), the chamber may be assumed to work in pure avalanche mode and the streamer probability becomes negligible. At higher voltage the streamers percentage grows rapidly and the chamber works in a sort of mixed mode: an increasing fraction of avalanche signals is accompanied by delayed streamer signals [10]. At a given streamer probability, the efficiency is higher in freon due to the higher gas density. In addition, the plateau region (defined here as the HV interval where efficiency is greater than 95% and streamer probability is less than 10%) is wider in freon.

Double gap efficiency and streamer probability under irradiation are shown in fig.s 7 for freon (fig. 7c) and argon (fig. 7d) respectively. Results with no source are shown again for sake of comparison. While there is a small loss of efficiency in freon, the effect is more relevant in argon where it is accompanied by a narrowing of the plateau.

The fast charge induced on the strip when the chamber is operated in avalanche mode has been measured in different working conditions, i.e.: source, no source, single gap, double gap. A summary of the average results is given in fig.s 8 for freon (8a) and argon (8b) respectively.

As we measure half of the fast induced charge, the results of the measurements must be multiplied by a factor 2. In the following we shall always refer to the total induced charge  $q_e = 2q_{meas}$ .

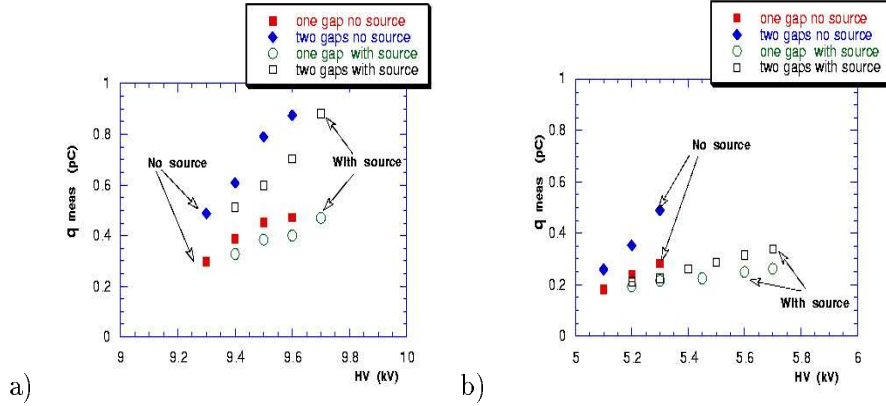


Figure 8: Average measured fast charge on the pickup electrode: a- freon; b- argon.

The chamber operated in freon exhibits twice the fast charge produced in argon; therefore the achievement of high efficiency in argon requires a more demanding front-end electronics or a lower discrimination threshold. The use of an electronegative gas such as  $C_2H_2F_4$  could lead to severe power consumption in the LHC background conditions. During the development of an avalanche, a sizeable amount of the produced electrons are trapped and do not further contribute to the multiplication process. It is a simple matter to show that the fast charge  $q_f$  induced on the pickup electrode is only a small fraction of the total charge  $q_e$  developed inside the gap and moved by the power supply. In avalanche mode, the fast visible charge is, at most, about 7% of  $q_s$ , in the case of non electronegative gases and becomes even smaller in the case of electronegative gases. Of course, the power consumption is determined by the total charge  $q_s$ . When an electronegative mixture is used, for a given signal on the pickup electrode more total charge is involved and the consumption is larger than that of a non electronegative mixture. We estimated the power consumption with the freon mixture by measuring the increment of the current drawn by the HV supply, when the chamber is operated under irradiation, compared to the current with no irradiation. In fig. 9a the power consumption for a single gap is plotted vs HV. The measurements refer to a situation in which only a small part of the RPC is irradiated.

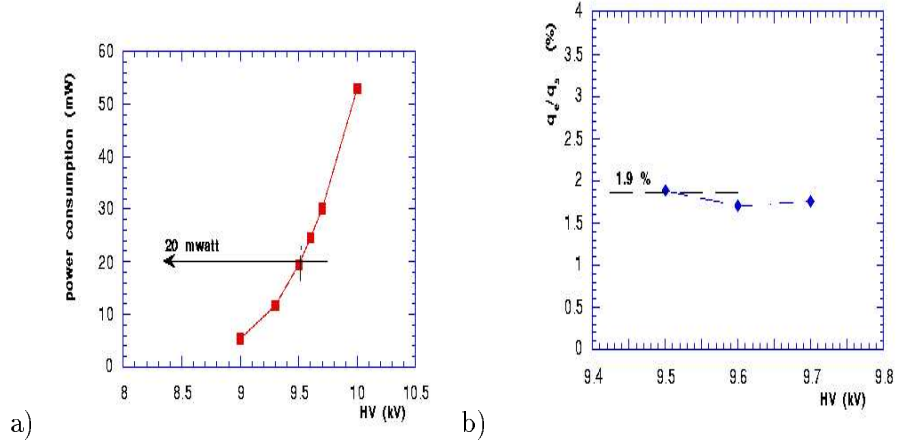


Figure 9: a- single gap power consumption for a 50cm x 50cm RPC under irradiation; b- ratio of the fast charge to the total charge for one single gap avalanche.

An estimate of the power consumption at the CMS background condition can be obtained by evaluating first the amount of total average charge  $q_s$  moved by the power supply when a single avalanche is developed in the gas. This can be computed as the increase of the single gap current, normalized to the counting rate, when the radioactive source is positioned above the chamber. At 9500 V we find  $q_s = 41$  pC, which is about 50 times larger than the corresponding fast charge induced on the pickup electrode.

The power consumption, for a  $1 \text{ m}^2$  chamber uniformly irradiated at an equivalent counting rate of  $100 \text{ Hz/cm}^2$ , can then be estimated as:

$$(41 \text{ pC}) \times (100 \text{ Hz/cm}^2) \times (10^4 \text{ cm}^2) \times (9500 \text{ V}) = 400 \text{ mW} \quad (2)$$

Therefore a  $1 \text{ m}^2$  double gap RPC operating in avalanche mode with  $C_2H_2F_4$  at the CMS background condition would dissipate less than a  $1 \text{ W/m}^2$ .

In fig. 9b, the ratio  $\frac{\text{fast charge } q_e}{\text{total charge } q_s}$  is plotted vs HV, showing that it decreases to about 2% due to the gas electronegativity, as compared to the typical 7% of non electronegative mixtures. The power consumption with argon mixture can also be evaluated. From fig. 8b, the fast induced charge is 0.2 pC at 5200 V, which is equivalent to 0.4 pC, if the strip termination is taken into account. On the other hand, the argon mixture is known to have negligible electronegativity. Therefore, being  $\alpha$  the first Townsend coefficient and  $d$  the gas gap, we can assume  $\alpha \cdot d \simeq 18$  in avalanche mode with moderate gas gain, obtaining  $q_s = \alpha d q_e = 0.4 \times 18 \simeq 7$  pC. In analogy to (1) we can evaluate 40 mW of power consumption.

However, a reduction of the power consumption by a factor 10 compared to freon, is only apparent, as the efficiencies of the two mixtures are not comparable (70% in argon, 95% in freon). A more realistic estimate can be performed by imposing equal efficiencies. By using the results shown in fig.s 7 and 9a we rather find a factor 5.

### 3.2 Comparison of the data to Montecarlo Simulations

In this section we compare the measured charge distribution to the prediction of a simulation based on a model for the mechanism of the signal formation. Its detailed description can be found in ref. [2]f. The model is based upon physical parameters such as the Townsend coefficient  $\alpha$  (number of ionizing encounters per unit length undergone by one electron), the attachment coefficient  $\beta$  (number of attaching encounters per unit length undergone by one electron) and the effective ionization coefficient  $\eta = \alpha - \beta$ .

The induced fast charge  $q_e$  and the total charge  $q_s$  are related by the simple formula:

$$\frac{q_e}{q_s} = \frac{k}{\alpha d} \quad (3)$$

where  $k$  depends upon geometrical and electrical factors such as, the relative dielectric constant  $\epsilon_r$  of the bakelite, the gas gap width  $d$  and the electrode thickness  $s$ :

$$k = \frac{\frac{\epsilon_r d}{s}}{\frac{\epsilon_r d}{s} + 2}$$

The values predicted for the physical parameters are:

$$\eta \simeq 9.2 \text{ mm}^{-1}, \alpha \simeq 18 \text{ mm}^{-1} \text{ in } C_2H_2F_4 \text{ at } 9500 \text{ V}$$

$$\eta \simeq 9.2 \text{ mm}^{-1}, \alpha \simeq \eta \text{ in argon at } 5200 \text{ V}$$

Using these values, the ratio  $q_e/q_s$  for the  $C_2H_2F_4$  based mixture can be evaluated from (3):

$$\frac{q_e}{q_s} = 1.9\%$$

A Montecarlo simulation has been implemented which included all possible effects in the avalanche multiplication inside an RPC, such as the fluctuations on the initial position and on the size of primary clusters and fluctuations on the total number of electrons.

Details on the structure of the programs can be found in [11]. Here we only briefly list the relevant steps of the simulation process:

1. The crossing of an ionizing particle through the RPC gap is simulated by generating along its path the primary clusters. From Poisson statistics the probability of finding the  $j$ -th cluster lying between  $x$  and  $x + dx$  is

$$P_j(x)dx = \frac{x^{j-1}}{(j-1)!} \lambda^j e^{-\lambda x} dx \quad (4)$$

$\lambda$  being the cluster density in the mixture.

The number of electrons  $n_j$  in the primary  $j$ -th cluster is generated either from experimental, if available, or theoretical distributions reported in the literature.

2. The fast charge  $q_e$  due to the avalanche originated by the  $j$ -th primary cluster is computed according to:

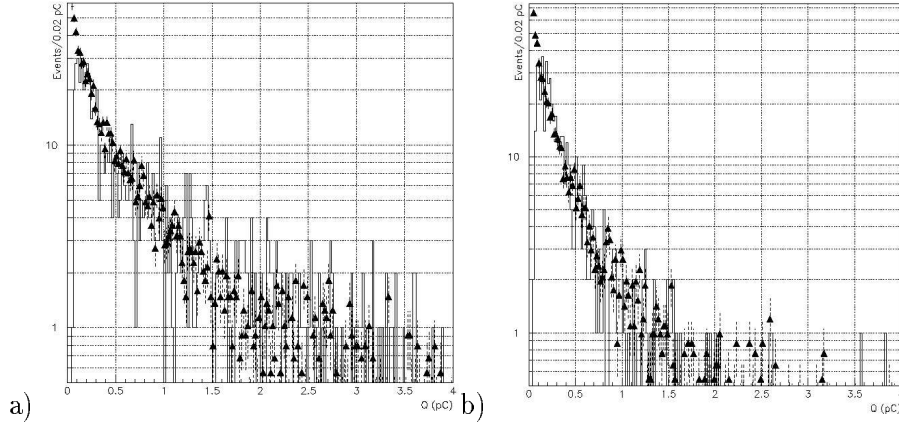


Figure 10: Comparison of Monte Carlo charge spectrum distributions to experimental data: a-  $C_2H_2F_4$  based mixture; b- argon based mixture.

$$q_e = \frac{k}{\eta d} Q_j g [e^{\eta(d-x_j)} - 1] \quad (5)$$

where  $Q_j = q_{el} n_j$  ( $q_{el}$  is the electron charge) and  $g$  is a factor which accounts for the fluctuation in the avalanche gain. It is determined by randomly extracting a number from an exponential distribution with average value equal to  $n_j e^{\eta(d-x_j)}$

3. The total fast charge  $q_e$  is obtained by summing the contributions of all clusters

Predictions for the charge distribution can be obtained by inserting in the simulation the parameters  $\lambda$  and  $\eta$  mentioned above.

By fitting the results of the simulation with the available experimental charge distributions, the properties  $\lambda$  and  $\eta$  of the used gas mixtures can be obtained.

The comparison of experimental and simulated charge spectra are shown in fig.s 10, for a 2 mm single RPC gap filled with  $C_2H_2F_4$  (fig. 10) and a  $3 \times 3mm$  multigap RPC (filled with argon), both operated at the knee of the efficiency plateau.

The agreement between the experimental data and simulations is fairly good. The Monte Carlo charge distributions in fig.s 10 do not take into account the experimental threshold ( $\simeq 100$  fC) for signal detection; therefore it extends to very low charge values where no signal was detected experimentally.

The use of heavy gases produces more charge on the pickup electrode (on average,  $\simeq 0.9$  pC for the single gap RPC and  $\simeq 0.5$  pC for the multigap RPC) and requires to operate the detector at higher threshold.

We find, however, large values for  $\lambda$ . This may be explained considering that the number of clusters/mm was extrapolated from known results for minimum ionizing particles only. However since the experimental tests were performed with high energy particles, we expect a larger energy loss and therefore larger values of  $\lambda$ .

## 4 Conclusions

Surface treatment of the internal bakelite electrodes is a necessary step to reduce noise and dark current of RPCs operated in streamer mode. The overall result seems to be the smoothness of the surface. However the absence of the oiling agent does not sensitively affect other parameters such as efficiency, cluster size and charge distribution. We proved that the effect of the linseed oil (i.e. the smoothness of the surface) can be obtained within the industrial process of the bakelite foil production. Chambers made by smoother surface bakelite and linseed oiled bakelite show similar performances. In no way oil treatment degrades the performances of an RPC at least when operated in streamer mode.

The study of double gap RPCs -operated in avalanche mode- under irradiation of a  $^{137}\text{Cs}$  source at an equivalent rate of  $500 \text{ Hz}/\text{cm}^2$  shows that environmental friendly freon mixtures seem to be more suitable than argon mixtures to reach high efficiency with limited streamer fraction. The power consumption, which could be an issue being  $\text{C}_2\text{H}_2\text{F}_4$  electronegative, is limited and acceptable for the LHC background running conditions.

Experimental charge spectra are well explained by a proper Montecarlo simulation. The model is a tool suitable to explain the physical process taking place in the RPC gaps during the development of the avalanche. A double gap geometry appears to be preferable to a multigap configuration. This aspect cannot be neglected, if one considers that pickup noise cannot be reduced at will, due to the large detector area. In our experience, this sets a lower limit to the threshold around 20 fC. The advantage of freon mixtures (greater average fast charge), which enables to reach high efficiency with relatively higher thresholds seems to be evident. Comparable efficiencies in argon mixtures would require much lower thresholds which could hardly be used.

## References

- [1] a- Proc. 2nd Int. Workshop on R.P.C. in Particle Phys. and Astroph., Sci. Acta **8**, 1 (1993); b- Proc. 3rd Int. Workshop on R.P.C.'s and Related Detectors, Sci. Acta **11**, 1 (1996);
- [2] a- M. Abbrescia et al., Sci. Acta **11**, 217 (1996); b- A. Di Ciaccio, Proc. EPS-ICHEP (Ed. J. Lemonne, C. Vander Velde, F. Verbeure. World Sci. 1996) p. 605; c- A. Di Ciaccio, Sci. Acta **11**, 263 (1996); d- E. Cerron Zeballos et al, Nucl. Instr. and Meth. **A367**, 388 (1995); e- C. Bacci et al., N.I.M. in Phys. Res., **A352**, 552 (1995); f- M. Abbrescia et al., *Properties of  $C_2H_2F_4$  based mixtures for avalanche mode operation of Resistive Plate Chambers*. CMS Note 1997/004, (sub. to N.I.M.);
- [3] R. Santonico and R. Cardarelli, N. I. M. **187**, 377 (1981);
- [4] a- P. Fonte, Sci. Acta **11**, 25 (1996); b- R. Cardarelli, R. Santonico, V. Makeev, Sci. Acta **11**, 11 (1996) c- I. Duerdoth et al, N. I. M. in Phys. Res. **A348**, 303 (1994); d- I. Crotty et al., N. I. M. in Phys. Res. **A337**, 370 (1994);
- [5] R.Cardarelli et al., N.I.M. in Phys. Res. **A333**, 339 (1993); b- C.Bacci et al., N.I.M. in Phys. Res. **A352**, 552 (1995);
- [6] *Ullmann's Encyclopedia of Industrial Chemistry*, Vol. **A10** (1994) p. 227.
- [7] a- J. Feder, *Fractals* (Ed. Plenum Pr, N.York, London, 1988); b- S. P. Ratti, *Introduction to Fractals in Physics* (Lecture Notes, 1997);
- [8] a- P. Vitulo, Private comm. at the December CMS week, 1996; b- M. Abbrescia et al., *Effect of the linseed oil treatment on the performance of the Resistive Plate Chambers*, CMS NOTE 1997/018; (to appear in N.I.M. in Phys. Res., 1997);
- [9] a- E.Cerron Zeballos et al., N.I.M. in Phys Res. **A367**, 388 (1995); b- M.Abbrescia et al., Nucl. Phys. **B44**, 289 (1995);
- [10] I.Duerdoth et al., N.I.M. in Phys. Res. **A348**, 303 (1994);
- [11] a- M.Abbrescia: *Resistive Plate Chambers in Avalanche Mode: a Comparison between Model Predictions and Experimental Results* (to be published in Proc. VIIth Pisa Meeting on Advanced Detectors, 1997); E.Cerron Zeballos, *Fluctuation within a Multigap RPC*, (to appear in N.I.M. in Phys. Res. 1997);